Effect of interstitial nitrogen on the structural and magnetic properties of $NdFe_{10.5}V_{1.5}N_x$

Jinbo Yang,[a] Bo Cui, Weihua Mao, Benpei Cheng, Jianian Yang, Bo Hu, and Yingchang Yang
Department of Physics, Peking University, Beijing 100871, People's Republic of China

Senlin Ge
Beijing University of Post and Communications, Beijing 100080, People's Republic of China

(Received 20 June 1997; accepted for publication 14 November 1997)

The $NdFe_{10.5}V_{1.5}N_x$ nitrides crystallize in the $ThMn_{12}$-type structure. The nitrogen atoms occupy interstitial sites, and their most important effects are on the crystal fields around the rare earth ion sites. The variation of anisotropy fields of $NdFe_{10.5}V_{1.5}N_x$ as a function of the nitrogen content x is presented. The crystal field interaction parameters are determined by using single-ion model. In the light of this study, high performance magnetic powders based on $NdFe_{10.5}V_{1.5}N_x$ were successfully prepared. © *1998 American Institute of Physics.* [S0021-8979(98)02305-6]

I. INTRODUCTION

The ternary $RFe_{12-x}M_x$ intermetallic compounds crystallizing in tetragonal $ThMn_{12}$-type structure can be stabilized when M=Ti, V, Cr, Mn, Mo, W, Al, or Si and x is in the range $1.0 \leqslant x \leqslant 4.0$.[1–3] Desirable effects of interstitial nitrogen atoms on the magnetic properties of $RFe_{12-x}M_xN_y$ compounds were reported.[4–7] The nitrogen atoms occupy the interstitial 2b sites,[8–10] which have an effect of increasing both Curie temperature by 200 K and the saturation magnetic moment of iron by 10%–20%. Moreover, a fundamental change in magnetocrystalline anisotropy of rare earth ions was achieved by introducing the interstitial nitrogen atoms. The rare earth ions, such as Nd, Tb, Dy, and Ho, present an easy axis with a large anisotropy field after nitrogenation. This change is of significant importance, since the origin of a high coercivity comes from a strong uniaxial anisotropy. In particular, due to the ferromagnetic coupling between light rare earth and iron, $NdFe_{12-x}M_xN_y$ nitrides emerge as a promising type of novel hard magnetic materials. The magnetic properties of the $NdFe_{12-x}M_x$ and their nitrides vary with the third element M. Among them, $NdFe_{12-x}V_xN_y$ possesses a higher Curie temperature and larger saturation magnetization. Obviously, it is of theoretical and technical significance to carry out a systematic investigation on the relationship of the crystallography structure, magnetocrystalline anisotropy, and hard magnetic properties with their nitrogen content in $NdFe_{10.5}V_{1.5}N_x$ nitrides.

II. EXPERIMENTAL AND CALCULATION METHODS

$NdFe_{10.5}V_{1.5}$ and $YFe_{10.5}V_{1.5}$ ingots were prepared by the arc melting of 99.9% pure materials in an argon atmosphere, followed by a heat treatment around 1000 °C for one week. The nitrogenation was carried out at 500–600 °C for several hours in high purity N_2 gas at atmospheric pressure. The magnetization curves of aligned samples were measured using vibrating sample magnetometer with a field of up to 20 kOe at room temperature. Crystal phase was identified by x-ray diffraction analysis with Cu K_α radiation. The anisotropy constants K_1 and K_2 are deduced from the fitting of magnetization curves perpendicular to the alignment direction using Sucksmith–Thompson method.[11] Theoretical calculation using the single-ion model was performed.

III. RESULTS AND DISCUSSIONS

A. Crystallographic structure

The typical x-ray diffraction patterns of $NdFe_{10.5}V_{1.5}N_x$ are presented in Fig. 1. All the compounds are identified to crystallize in $ThMn_{12}$-type tetragonal structure (so-called 1:12 phase). The parent alloy before nitrogenation is of single phase without any magnetic impurity, which can be also verified by thermomagnetic curves shown in Fig. 2. However, a little amount of α-Fe appears when nitrogen content increases. All the x-ray diffraction peaks of $NdFe_{10.5}V_{1.5}N_x$ shift to lower angle when $x \leqslant 2.0$. This is evidence that nitrogen atoms enter into interstitial sites and result in a lattice expansion. The positions of diffraction peaks remain unchanged when $x > 2.0$, indicating the nitrogen atoms that do not enter the interstitial sites any more, and the precipitation of α-Fe and neodymium nitrides become visible in the meantime. The lattice parameters a and c, unit cell volume V, as well as relative change in unit cell volume $\delta V/V$ of $NdFe_{10.5}V_{1.5}N_x$ are summarized in Table I.

A number of neutron diffraction studies on $YFe_{11}TiN_x$, $YFe_{10}V_2N_x$, and $YFe_{10}Mo_2N_x$ or $YFe_{11}MoN_x$ have been made previously.[8–10] All studies present the same conclusion that nitrogen atoms occupy the octahedral $2b$ interstitial sites. Accordingly, full occupation of $2b$ sites in the case of $NdFe_{10.5}V_{1.5}N_x$ leads to a composition of $NdFe_{10.5}V_{1.5}N_{1.0}$. However, the experimentally estimated nitrogen content x in $NdFe_{10.5}V_{1.5}N_x$ ranges from 0 to as large as 2.7, which is much higher than the theoretical value of one nitrogen atom per formula unit. This fact suggests that the nominal nitrogen

[a]Electronic mail: jbyang@ibm320h.phy.pku.edu.cn

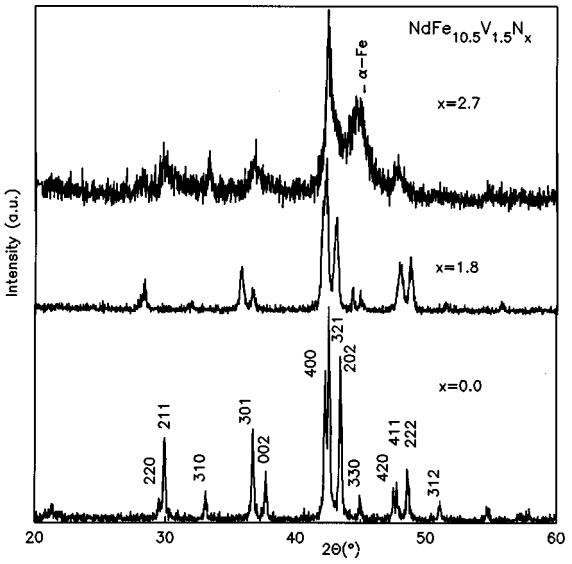

FIG. 1. The x-ray diffraction patterns of the $NdFe_{10.5}V_{1.5}$ and $NdFe_{10.5}V_{1.5}N_x$.

content is much larger than the nitrogen occupancy number on $2b$ site. The nominal nitrogen content is obtained by weighting the sample before and after nitrogenation. So the weight included everything gained during nitrogenation such as N in the particle surface (physical absorption) and in the bulk, or factors other than N absorption.[10] This may offer an explanation to why different studies have reported different nitrogen content values, while corresponding lattice expansion and magnetic properties were not so different. As a result, it is reasonable to assume that the nominal composition of $NdFe_{10.5}V_{1.5}N_2$ with $x=2.0$ corresponds to a nearly full occupation on the $2b$ site, which has the largest volume expansion. When the nominal nitrogen content $x>2.0$, an over nitrogenation occurs with an evidence of decomposition.

TABLE I. The crystal lattice parameters of $NdFe_{10.5}V_{1.5}N_x$.

x	a (Å)	c (Å)	V (Å^3)	$\delta V/V$ (%)
0.0	8.5411	4.7540	344.4	0.0
0.6	8.5943	4.7729	352.5	2.4
1.1	8.6187	4.8136	357.5	3.8
1.5	8.6174	4.8143	358.1	4.0
1.8	8.6120	4.9000	363.4	5.5
2.0	8.6070	4.9070	363.5	5.5
2.2	8.5910	4.9180	363.0	5.4
2.7	8.5640	4.8980	359.2	4.3

B. Magnetocrystalline anisotropy

The magnetization curves of $NdFe_{10.5}V_{1.5}N_x$, parallel and perpendicular to the alignment direction measured at room temperature are plotted in Fig. 3. The saturation magnetizations, anisotropy constants K_1 and K_2, as well as anisotropy fields H_a are summarized in Table II. A significant dependence of magnetocrystalline anisotropy on nitrogen content is observed. The magnetocrystalline anisotropy of $NdFe_{10.5}V_{1.5}N_x$ arises from the contributions of both the Nd sublattice and the Fe sublattice. The contribution from Fe sublattice can be estimated experimentally by fitting the magnetization curves along the hard magnetization direction of aligned samples of $YFe_{10.5}V_{1.5}N_x$. The values of K_1 and K_2 for the Fe sublattice are shown in Fig. 4. The Fe sublattice possesses always an easy axis both before and after nitrogenation. The values of anisotropy constant decrease only slightly with increasing nitrogen content. However, no big change occurs upon nitrogenation. So it is evident that a drastic change takes place in the Nd sublattice anisotropy with nitrogenation.

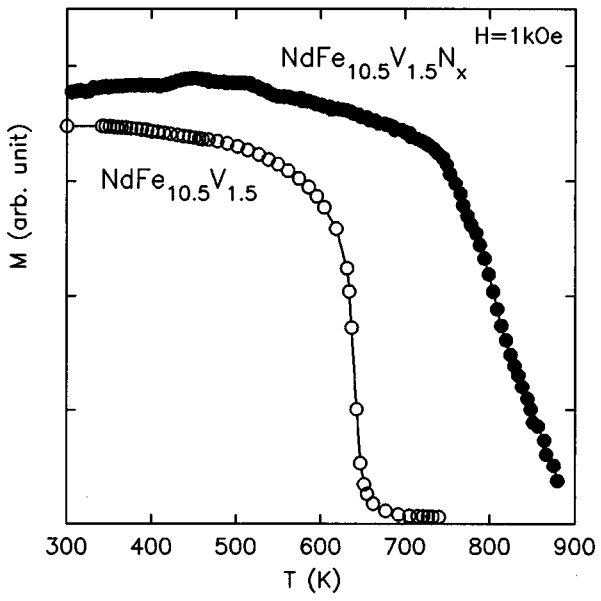

FIG. 2. The thermomagnetic curves of the $NdFe_{10.5}V_{1.5}$ and $NdFe_{10.5}V_{1.5}N_x$.

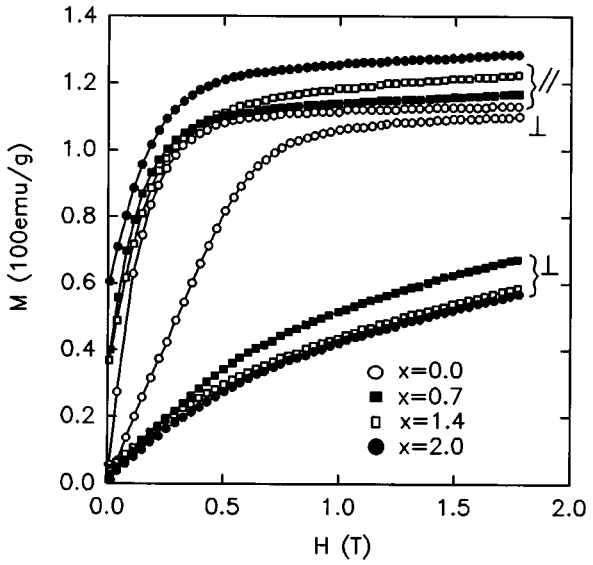

FIG. 3. The room temperature magnetization curves of the magnetically oriented powder samples of the $NdFe_{10.5}V_{1.5}N_x$.

TABLE II. The intrinsic magnetic properties of the $NdFe_{10.5}V_{1.5}N_x$ powders.

x	M_s (emu/g)	K_1 (10^7 erg/cm^3)	K_2 (10^6 erg/cm^3)	H_a (kOe)
0.0	114.1	0.13	0.47	0.5
0.7	120.6	3.34	5.80	7.3
1.4	126.0	3.52	6.24	9.9
2.0	131.5	3.80	7.07	10.4
2.7	132.1	−0.11	33.30	···

TABLE III. Crystal-field parameters of the rare-earth sublattice B_{nm}(K).

x	B_{20}	$B_{40}\times10^{-3}$	$B_{44}\times10^{-3}$	$B_{60}\times10^{-5}$	$B_{64}\times10^{-5}$
0.0	0.80	0.43	−4.34	1.48	2.15
0.2	−0.64	−1.83	−3.73	−23.23	1.86
0.4	−2.09	−4.09	−3.12	−47.95	1.58
0.6	−3.54	−6.31	−2.51	−72.66	1.30
0.8	−4.99	−8.61	−1.89	−97.37	1.02
1.0	−6.43	−10.87	−1.28	−122.1	0.74

Since the aspherical orbital wave function of the $4f$ electrons interacts strongly with crystal field, the Nd ions make a great contribution to the anisotropy of $NdFe_{10.5}V_{1.5}N_x$. The anisotropy energy with a tetragonal symmetry can be phenomenologically expressed as

$$E(\theta)=K_0+K_1\sin^2\theta+K_2\sin^4\theta+\cdots, \tag{1}$$

where θ is the angle between the c axis and the magnetization vector. As the $4f$ electrons of rare-earth are well localized, the contribution of the Nd sublattice to the magnetocrystalline anisotropy can be calculated by using the single-ion model. The perturbation Hamiltonian is

$$H_{4f}=H_{cf}+H_{ex}, \tag{2}$$

where H_{cf} is the crystal-field Hamiltonian, while H_{ex} is the exchange interaction Hamiltonian and can be written as

$$H_{ex}=g_J\mu_B\mathbf{H}_m\cdot\mathbf{J}, \tag{3}$$

where H_m is molecular field estimated by fitting the saturation magnetization temperature curves of the Nd sublattice obtained from those of $NdFe_{10.5}V_{1.5}N_x$ and $YFe_{10.5}V_{1.5}N_x$. $NdFe_{10.5}V_{1.5}N_x$ retains the $ThMn_{12}$-type tetragonal structure with nitrogen atoms occupying the 2b interstitial sites. The Nd sublattice in the $ThMn_{12}$-type structure possesses I4/*mmm* point symmetry, so the crystal-field Hamiltonian is expressed as

$$H_{cf}=B_{20}O_{20}+B_{40}O_{40}+B_{44}O_{44}+B_{60}O_{60}+B_{64}O_{64}, \tag{4}$$

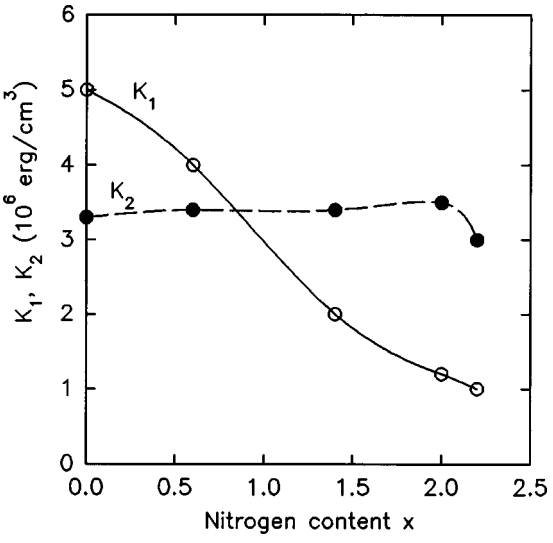

FIG. 4. The anisotropy constants of Fe sublattice in $YFe_{10.5}V_{1.5}N_x$.

where $B_{kq}=\theta_n\langle r^n\rangle A_{kq}$, $\theta_n=\alpha_J$, β_J, and γ_J for $n=2$, 4, and 6, respectively; $\langle r^n\rangle$ are expectation values of r^n for the $4f$ shell, A_{kq} are the crystal-field coefficients, and O_{kq} are the Stevens equivalent operators. The $4f$ electrons lie within the $5s$ and $5p$ orbits and are strongly screened from the surrounding ions. Therefore, a set of screening factors ($\sigma_{2,4,6}$) are introduced to represent this effect. Finally the perturbation Hamiltonian is

$$\begin{aligned}H_{4f}=&(1-\sigma_2)B_{20}O_{20}+(1-\sigma_4)(B_{40}O_{40}+B_{44}O_{44})\\&+(1-\sigma_6)(B_{60}O_{60}+B_{64}O_{64})\\&+g_J\mu_BH_m(J_x\sin\theta+J_z\cos\theta).\end{aligned} \tag{5}$$

To calculate the crystal-field parameters, 16 rare-earth ions, 28 iron ions, and 16 nitrogen ions are considered as ligands. Because the farther ions are shielded not only from the outer electrons of Nd but also by the ''sea'' of free electrons and nearer ions, hence, their contribution is negligible. The free energy density is

$$E(\theta)=-NKT\ln(\Sigma e^{-E_i/KT}), \tag{6}$$

where N is the density of Nd^{3+} ions, $T=295$ K, and E_i is the eigenvalue of H_{4f} and can be obtained by solving the following secular equation:

$$|\langle LSJM'|H_{4f}|LSJM\rangle-E_i\delta_{M'M}|=0, \tag{7}$$

where $L=3$, $S=3/2$, $J=9/2$, and M', $M=-9/2$, $-7/2$, ..., $9/2$. Through solving Eq. (7), a set of crystal-field parameters of Nd^{3+} are obtained. The results are listed in Table III, and corresponding second order crystal-field coefficient A_{20} as a function of nitrogen content is presented in Fig. 5. The calculated results indicate that the second order crystal-field parameter is dominant in determining the anisotropy of the rare-earth sublattice as higher order items are so small in the $NdFe_{10.5}V_{1.5}N_x$ series. The change in the sign of A_{20} from negative to positive after nitrogenation is important. Due to this change, the c axis becomes the easy magnetization direction for the $NdFe_{10.5}V_{1.5}N_x$ nitrides form 0 K to Curie temperature.

Since the contribution from neighbor nitrogen ions to the second-order crystal-field coefficient A_{20} are positive and large while the contribution from neighbor rare-earth ions are negative and smaller, this results in a change in the sign of A_{20} from negative in the host compounds to positive in the nitrogen interstitial modified compounds. Therefore the rare-earth sublattice anisotropy changes completely. All the rare-earth ions whose second order Stevens coefficient α_J are negative, such as Nd^{3+}, prefer an easy axis. As shown in

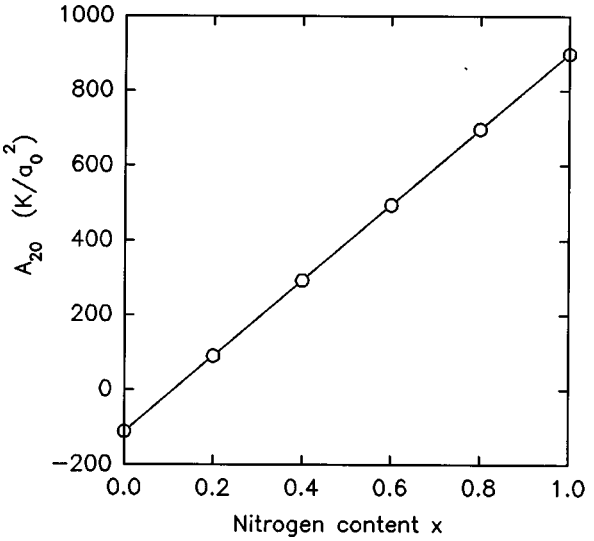

FIG. 5. The second-order crystal-field coefficients A_{20} as a function of nitrogen content.

Fig. 5, A_{20} increases linearly as the nitrogen content increases. This is consistent with the experimental data, see Fig. 3. In order to compare the measured values with the calculation results, it is assumed that x is equal to 1.0 for the sample with a nominal composition of $NdFe_{10.5}V_{1.5}N_2$ whose unit cell volume does not increase further, which means $2b$ sites were fully occupied. Consequently, the x of other samples is assumed to be proportional to the relative change in the unit cell volume by comparing with $NdFe_{10.5}V_{1.5}N_2$. The x denotes the average occupancy number of nitrogen in the $2b$ site. The theoretical values of K_1 and K_2 (Fig. 6) are in good agreement with the experimental data except a deviation in high nitrogen content region. This is partly because the nitrogen content of the sample cannot be estimated very accurately. We can conclude that with a pure 1:12 phase and full nitrogenation in the $2b$ site, a uniaxial anisotropy field of up to 13 T at room temperature will be expected as indicated in Fig. 6.

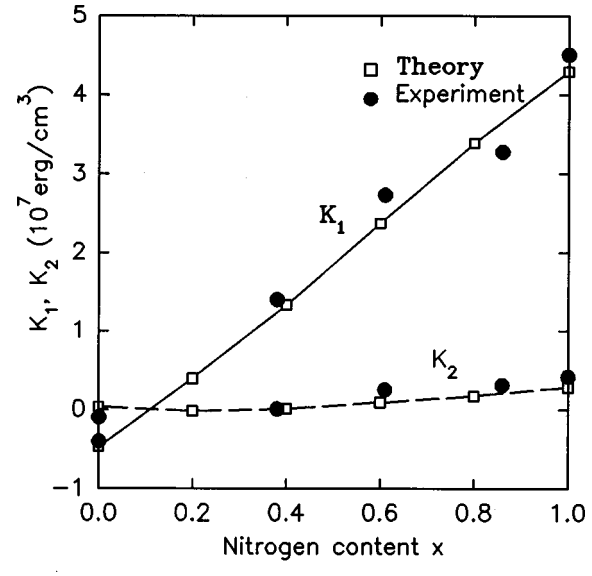

FIG. 6. The anisotropy constants of Nd^{3+} ions in $NdFe_{10.5}V_{1.5}N_x$.

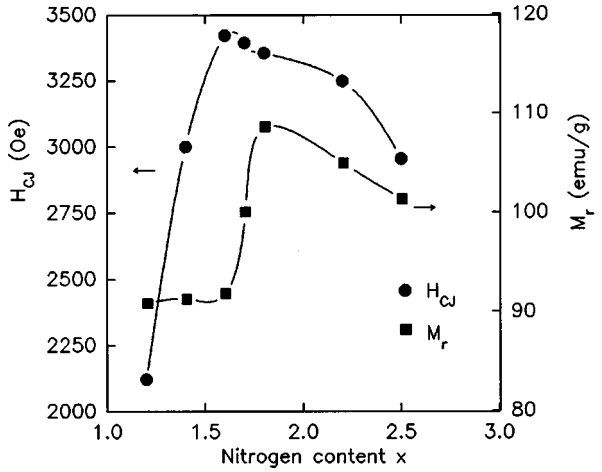

FIG. 7. The dependence of coercivity and remanent magnetization on nitrogen content of $NdFe_{10.5}V_{1.5}N_x$.

C. Permanent magnetic properties

An easy axis with a strong anisotropy field is prerequisite for a large coercive force. Consequently, the change in the sign of A_{20} allows $NdFe_{10.5}V_{1.5}N_x$ to be available for permanent magnet applications, and a proper nitrogenation process is a key leading to success in manufacturing high performance magnets based on the $NdFe_{10.5}V_{1.5}N_x$ compounds. Figure 7 shows the variation of coercive force ${}_iH_c$ and remnant magnetization M_r as a function of x for $NdFe_{10.5}V_{1.5}N_x$, where x is the nominal nitrogen content estimated by gravity. All powders were made by using the same host alloy without milling after nitrogenation. A maximum in ${}_iH_c$ and M_r is observed around $x=1.8$. Together with the x-ray diffraction data it is believed that under this value the nitrogenation is not sufficient and over this value a decomposition occurs. The impurities are harmful to the

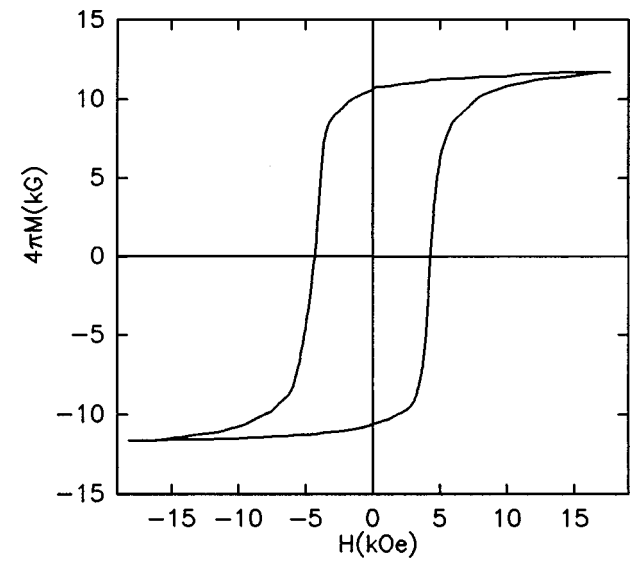

FIG. 8. The hysteresis loop of the epoxy-bonded $NdFe_{10.5}V_{1.5}N_x$ powders.

magnetic properties. Actually, a high performance powder of $NdFe_{10.5}V_{1.5}N_{1.7}$ with ${}_iH_c=4.3$ kOe, $B_r=10.8$ kG, and $(BH)_{max}=17.2$ MGOe was obtained by optimizing the nitrogenation and milling process. Its hysteresis loop is presented in Fig. 8. Finally, the temperature dependence of coercivity of the $NdFe_{10.5}V_{1.5}N_x$ powders was determined by measuring temperature dependence of the hysteresis loops in a temperature range from room temperature to 450 K. The temperature coefficient of coercivity is smaller than that of $Nd_2Fe_{14}B$ magnets. Compared to the commercial Nd–Fe–B powders, they have a moderate coercive force, but a larger maximum energy product, and suitable for some practical applications.

IV. CONCLUSIONS

The experimental investigation showed that nitrogenation of $NdFe_{10.5}V_{1.5}$ will enhance the magnetocrystalline anisotropy of this compound. Theoretical results of anisotropy constants are well consistent with the experimental values. It is found that the contribution of neighbor nitrogen ions to the second order crystal-field coefficient A_{20} are positive and larger, while the contribution of neighbor rare-earth ions are negative and smaller. The former increases linearly and gives rise to a linear increase of K_1 with increasing nitrogen content. For the fully nitrogenated samples with a strong uniaxial anisotropy field, $NdFe_{10.5}V_{1.5}N_x$ is promising for permanent magnet applications. In fact, anisotropic magnetic powders with $H_c=4.3$ kOe $B_r=10.8$ kG, and $(BH)_{max}=17.2$ MGOe have been obtained.

[1] Y. C. Yang, B. Kebe, W. J. James, J. Deportes, and W. Yelon, J. Appl. Phys. **52**, 2077 (1981).
[2] K. H. Bushow, J. Appl. Phys. **63**, 3130 (1988).
[3] K. Ohashi, Y. Tawara, R. Osugi, and M. Shimao, J. Appl. Phys. **64**, 5714 (1988).
[4] Y. C. Yang, X. D. Zhang, Q. Pan, L. S. Kong, and S. L. Ge, Appl. Phys. Lett. **58**, 2042 (1991).
[5] Y. C. Yang, X. D. Zhang, S. L. Ge, Q. Pan, L. S. Kong, H. L. Li, B. P. Cheng, J. L. Yang, Y. F. Ding, B. S. Zhang, and C. T. Ye, J. Appl. Phys. **70**, 6001 (1991).
[6] W. Gong and G. C. Hajipanayis, J. Appl. Phys. **73**, 6245 (1993).
[7] H. Sun, M. Akayma, K. Tatami, and H. Fujii, Physica B **183**, 33 (1993).
[8] Y. C. Yang, X. D. Zhang, L. S. Kong, Q. Pan, J. L. Yang, Y. F. Ding, B. S. Zhang, and C. T. Ye, Solid State Commun. **78**, 313 (1991).
[9] W. B. Yelon and G. C. Hadjipanayis, IEEE Trans. Magn. **28**, 2316 (1992).
[10] H. Sun, Y. Morij, H. Fujii, M. Akayama, and S. Funahashi, Phys. Rev. B **48**, 13 333 (1993).
[11] W. Sucksmith and J. E. Thomposon, Proc. R. Soc. London, Ser. A **225**, 362 (1954).